MONITORING OF TIMBER STRUCTURES BY FIBER-OPTIC SENSORS: CONCEPT AND FIRST RESULTS

ÜBERWACHUNG VON HOLZTRAGWERKEN MITTELS FASEROPTISCHER SENSOREN: KONZEPT UND ERSTE ERGEBNISSE

Aaron Münzer, Gerhard Dill-Langer

Materials Testing Institute (MPA), University of Stuttgart, Otto-Graf-Institute

SUMMARY

The extended range of timber constructions also to high-rise buildings or infrastructural buildings leads to a demand for structural monitoring methods with regard to a reliable detection of possible damage processes at an early stage. In a recently started research project it is investigated to what extent laser backscattering in fiber-optic sensors is suitable for spatially resolved strain measurement in large timber structures and to what extent this method can detect damage and separate it from other strain components such as creep or moisture movements. In a first step, the application of the test method to full-scale glulam structures including growth-related discontinuities such as knots is investigated.

ZUSAMMENFASSUNG

Der erweiterte Einsatzbereich des Holzbaus auch auf Hochhäuser oder Infrastrukturbauwerke führt zu vermehrten Nachfragen nach Methoden der Bauwerksüberwachung im Hinblick auf eine zuverlässige Erfassung von möglichen Schädigungsvorgängen in einem frühen Stadium. In einem kürzlich begonnenen Forschungsprojekt wird untersucht, inwieweit sich die Messmethode der Laserrückstreuung in faseroptischen Sensoren zur ortsaufgelösten Dehnungsmessung in großen Holzkonstruktionen eignet und inwieweit sich mit dieser Methode Schädigungen detektieren und von anderen Dehnungsanteilen wie z.B. Kriechen oder Feuchtebewegungen trennen lassen. In einem ersten Schritt wird die Anwendung der Messtechnik auf vollmaßstäbliche Brettschichtholzbauteile einschließlich der wuchsbedingten Ungänzen wie z. B. Äste untersucht.

1. INTRODUCTION

For years, timber engineering has not only shown a positive and increasingly dynamic development in terms of numbers, but is also increasingly expanding into areas which in the past were almost exclusively reserved for other material classes such as steel or reinforced concrete. Examples of this are multi-story structures even beyond the high-rise limit, structures with high traffic loads such as parking garages and infrastructure structures such as heavy-duty bridges. This trend is associated with innovations such as high-strength wood-based materials like laminated veneer lumber made of hardwoods and new connection techniques. In conjunction with the new fields of application, the circle of users is also expanding to include more institutional investors, who are more frequently asking critical questions about the long-term stability of timber structures even under unfavorable boundary conditions. In addition to a number of advantages such as the very good CO_2 balance, favorable conditions for a high degree of prefabrication and the associated very short construction times and the excellent weight-related strength properties, there are also potential weaknesses of the timber constructions: These include, above all, the pronounced anisotropy associated with a clear tendency to cracking under transverse tensile and shear stresses and the sensitivity of timber constructions to unfavorable moisture effects. For structures with low redundancy, at critical points such as joints, notches or openings, or when using new wood-based materials that have not yet been tested for a long time period, the question of possible structural monitoring is therefore increasingly being raised, in which incipient damage – e.g. due to microcrack formation – is detected at an early stage in order to enable countermeasures to be taken and thus significantly extend the service life of the structure.

Due to the predominantly (quasi-) brittle nature of the failure of wood and wood-based materials, monitoring by means of global deformation measurement – in contrast to e.g. metallic materials – is usually not applicable, since major deformations only occur at a very late stadium, sometimes even simultaneously with complete structural failure. Local strain measurements, on the other hand, can in principle be used to detect and further predict damage processes. Methods available today, such as strain measurement with strain gauges, are limited to a few predefined measuring points and, if extended to cover a larger area with many measuring points, entail considerable costs and installation effort for the strain gauge sensors, which can only be used once.

By means of photogrammetric / digital image correlation methods on the other hand, a complete strain measurement of entire component surfaces is possible with comparatively little effort, although both the spatial resolution and the strain resolution tend to decrease with the total area covered. In addition, certain surface conditions and, above all, unobstructed optical accessibility are always required for the camera recordings.

An alternative method of spatially resolved strain measurement that has been further developed in recent years involves the use of optical fibers that are bonded to the surface of the component to be monitored. By analyzing coupled laser light pulses, highly accurate and very finely spatially resolved strain measurements can be performed in real time – even for very long fiber lengths of up to 100 meters.

Regarding fiber-optic strain measurement, two concepts can be distinguished: Quasi-distributed measuring sensors and truly distributed measuring sensors. In both cases, the alteration of backscattered light in a fiber caused by either stress- or temperature-induced physical expansion or contraction of the specimen to which the fiber is attached is used for the derivation of strain information; however, crucial differences exist between the two, which significantly impact their capability and aptitude for different applications:

Quasi-distributed optical sensors are most commonly realized via so-called fiber Bragg gratings (FBG). These are microstructures of 5-10 mm length consisting of several evenly spaced etchings that are inscribed to the core of an optical fiber by exposure to a UV laser [1]. These microstructures alter the refractive index of the fiber core in this specific segment of the fiber, making it reflect only a narrow range of wavelengths. Whenever the optical fiber is elongated or compressed, the distance between the gratings changes and so does the spectrum of reflected wavelengths. The interrogator system detects this shift in reflected wavelengths and converts it into strain information.

FBG sensors have successfully been applied in various fields of timber engineering research within recent years, as for example by Claus et al. [2], who performed pull-out tests of self-tapping timber screws using a specially prepared measurement screw equipped with an inserted fiber-optic sensor containing 19 FBGs, enabling for the first time the accurate measurement of force distribution inside a screw during pull-out action and thus delivering an impressive display of the versatility of fiber-optic sensors in the context of laboratory and materials testing.

However, it is especially the evaluation of suitability of FBG sensors for the monitoring of timber structures that has drawn increased attention: Franke et al. [3] developed solutions for the implementation of FBG-based optical sensors in the wood industry to monitor the moisture content of timber building components based on strain measurement, especially addressing some wood-specific issues such as extreme swelling and shrinkage rates exceeding the strain capacity of conventional optical fibers many times; Marsili et al. [4] explored the potential of FBG sensors for the monitoring of historical timber buildings after reinforcement, i.e. assessing the success of beam reinforcement measures by comparing strain values before and after the procedure.

Although FBG-based measurement sensors or systems operate with optical fibers and thus share some of their unique benefits, such as e.g. resistance to harsh chemical, high temperature and high voltage environments, high measurement accuracy independent of sensor length as well as minimal cabling, at the same time they entail the same drawback as conventional electronic strain gauges in that they can only cover discrete locations of a specimen or building element. Therefore, information can only be increased by increasing the number of sensors and/or FBGs, resulting in high cost and effort. Furthermore, the observation of unexpected (strain) events is dependent on whether or not the distinct area is covered by an FBG and since crack formation in timber building elements, however, is a very local phenomenon, FBG strain monitoring of large-scale building components exhibits at the least a high degree of uncertainty or, in the worst case, a potential for data misinterpretation.

Truly distributed measuring sensors on the other hand are able to measure continuously along the whole length of the optical fiber as they rely simply on backscatter portions inherent to the fiber material itself. One of three different backscatter phenomena that occur in optical fibers is the so-called Rayleigh scattering, which is emitted by virtually every point of the fiber due to local defects, natural refractive index variations and wave conductor disturbances [5]. Any elongation or compression of the fiber induced by physical stress or temperature results in local modification of the fibers' unique Rayleigh backscatter pattern, which then, analogous to FBG-based sensors, is used to detect, localize and quantify said changes in the fibers' strain state.

As for FBG-based sensors, structural monitoring by means of truly distributed optical strain measurement has so far especially been employed in steel and concrete construction [1]; Schmidt-Thrö et al. [6] and Henault [7] et al. for example present respective laboratory and in-situ investigations of reinforced concrete structures. However, as of recent, also different approaches and concepts for monitoring of timber and timber-concrete structures using truly distributed optical sensors have been investigated: Teguedy et al. [8] present investigations on the early-age behavior of timber-concrete-composite slabs, including wet and dry curing phases, by embedding optical fiber sensors into both, the freshly poured concrete part as well as the cross-laminated timber (CLT) part of the slabs during manufacture. Among other findings, the strain development in both concrete and CLT could be used to track a shift in position of the neutral axis in the timber cross-section due to concrete shrinkage, providing a useful indicator of the "mechanical quality" of a timber-concrete-composite slab. Frohnmüller et al. [9] focused on approaches for monitoring the bondline integrity of adhesively joined timber-concrete-composite slabs using fiber-optic sensors placed directly between the CLT and concrete components prior to bonding, with the goal of detecting strain irregularities pre-indicating eventual failure of the bondline/element when subjected to 4-point bending. The experiments clearly demonstrate that a continuous strain monitoring of timber building elements has to consider growth-related discontinuities on the surface in the vicinity of the fiber-optic sensor, as their individual stress-strain behavior can differ considerably from that of clear wood, leading to challenges in measurement data interpretation. Finally, Jockwer et al. [10] present the implementation of truly-distributed fiber-optic strain measurement within the monitoring concept of a 15-storey timber-hybrid office building, investigating in specific the deformation behavior of the columns during the several months long construction phase. Therefore, selected column elements from the 1st to 8th floor of the building, made of beech laminated veneer lumber or spruce glued-laminated timber, were prepared with fiber-optic sensors attached parallel to the columns' length axes and strain measurements were taken after the completion of every new storey, showing the gradual increase in compressive strain not only subject to the changing load situations but to temperature and humidity fluctuations on the building site as well.

In a recently started ZIM research project the possibilities of using spatially resolved strain measurements by use of optical fiber sensors to detect possible damage in wood structures are investigated. The main challenge is how to separate the

non-linear, damage-relevant strain components from strain components due to other causes (e.g. creep or moisture strains). In the first step, however, which is the subject of this paper, the fiber-optic measurement methodology must first be examined with regard to its applicability to solid wood materials on a full component scale.

2. MATERIAL AND METHODS

The measurements were carried out with a glued-laminated timber beam from Norway spruce of strength class GL30h according to EN 14080 [11] with cross-sectional dimensions $w \cdot h = 120 \cdot 450$ mm² and a total length of $l = 3500$ mm. The beam was composed of 10 laminations with a thickness of $t_l = 41$ mm.

Two fiber-optic sensors (FOS) consisting of polyimide-coated single-mode optical fibers, each with a total sensor length of 15 m, were prepared for the measurements. The sensor fibers were spliced to a sensor interface and then connected to the interrogator unit. This unit sends laser pulses through the fiber and detects the Rayleigh back scatter signal from which the spatially resolved strain is derived. The spatial resolution was 0,65 mm and the measurement frequency 5 Hz, i.e. in every second 110 000 strain data are stored for each sensor.

The narrow sides of the two upper-most lamellas (No. 1 and 2) as well as the two lower-most lamellas (No. 3 and 4) of the GLT beam were equipped by the fiber-optic sensors on both sides “A” and “B” of the beam, resulting in eight “measuring segments” of $l_{FOS,gage} = 3500$ mm each and a total sensor coverage length of $l_{FOS,tot} = 8 \cdot 3500$ mm = 28 m. The gage denominations contain beam side (A or B) and lamella no. (1 to 4), resulting in segments A1, A2, B1 and B2 covering the two upper-most lamellas in the bending-compression zone and segments A3, A4, B3 and B4 covering the two lower-most lamellas in the bending-tension zone. Segments A1-B2 in the bending-compression zone were realized by fiber-optic sensor FOS-1 and segments A3-B4 in the bending-tension zone by fiber-optic sensor FOS-2. Fig. 1 schematically shows the arrangement of the optical fibers on the beam. The optical fiber sensors were glued to the whole length of the respective lamination irrespective of local defects such as knot or fissures.

For validation of the optical fiber measurements, a total of four electronic strain gauges (linear type, length of the measuring grid: 15 mm) were installed closely to the optical fibers. For simplicity, the electronic strain gauges are labelled ac-

cording to the optical fiber gage that they are installed next to it, resulting in electronic strain gauges A3 and A4 positioned at mid-span (x =1750 mm) and strain gauges B3 and B4 positioned approximately at one third-way point (x = 1145 mm). It was taken care to place strain gauges exclusively on clear wood parts of the lamellas without knots or other obvious defects for optimal comparability with the fiber-optic measurements at the respective locations. All electronic strain gauges were glued onto the lamellas using a one-component cyanoacrylate adhesive.

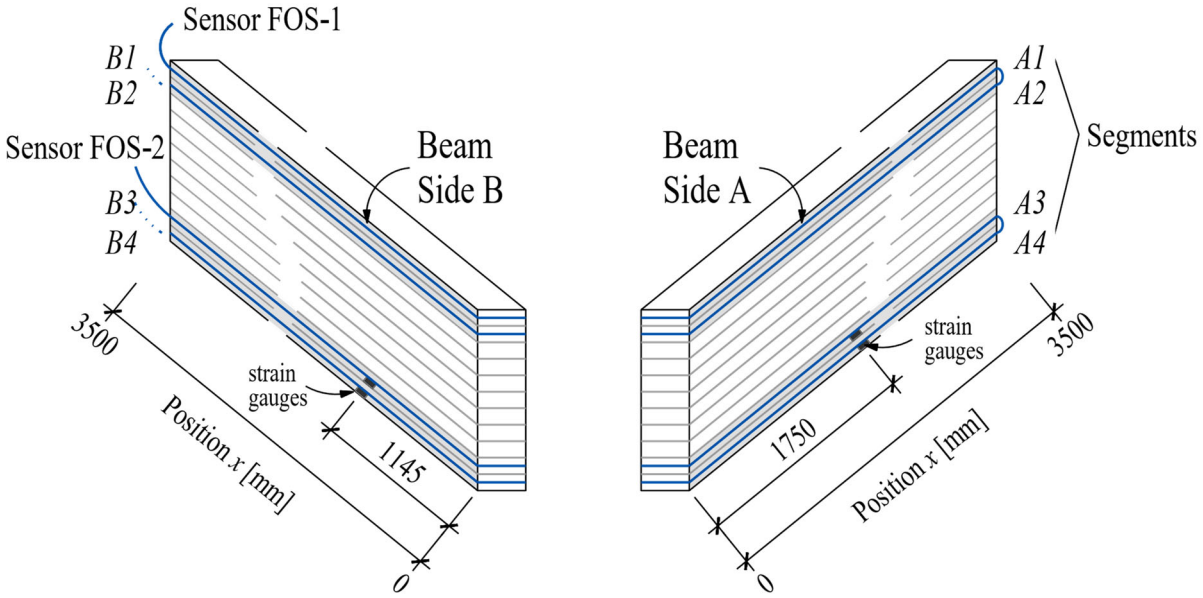

Fig. 1: Overview of the glulam specimen, the location and the labelling of the sensors

The GLT beam equipped with the different strain sensors was tested in a three-point bending configuration sketched in Fig. 2. The GLT beam was placed on rolling supports and steel plates. The load was introduced in mid-field at $l/2$ = 1750 mm through a steel plate resulting in a symmetric distribution of internal section forces M and V. Fig. 3a shows a photographic view of the test set-up and Fig. 3b gives a detailed view of the fiber-optical sensors and the electric strain gauges.

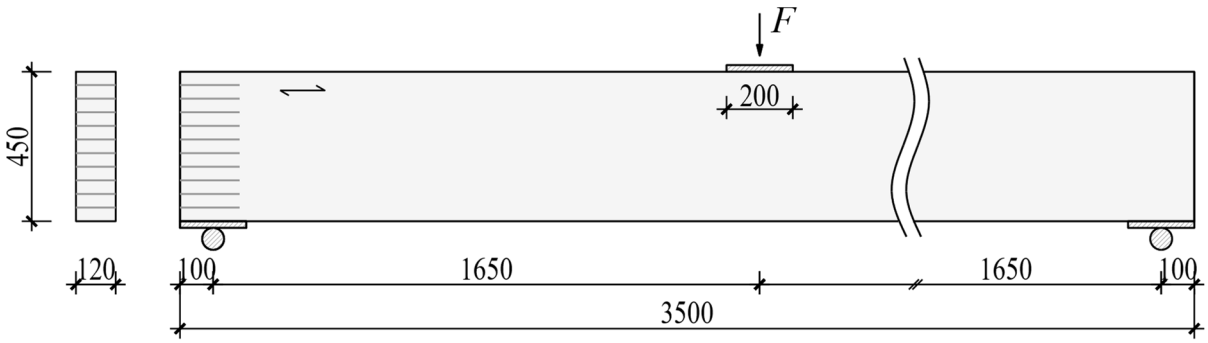

Fig. 2: Sketch of the three-point bending test setup

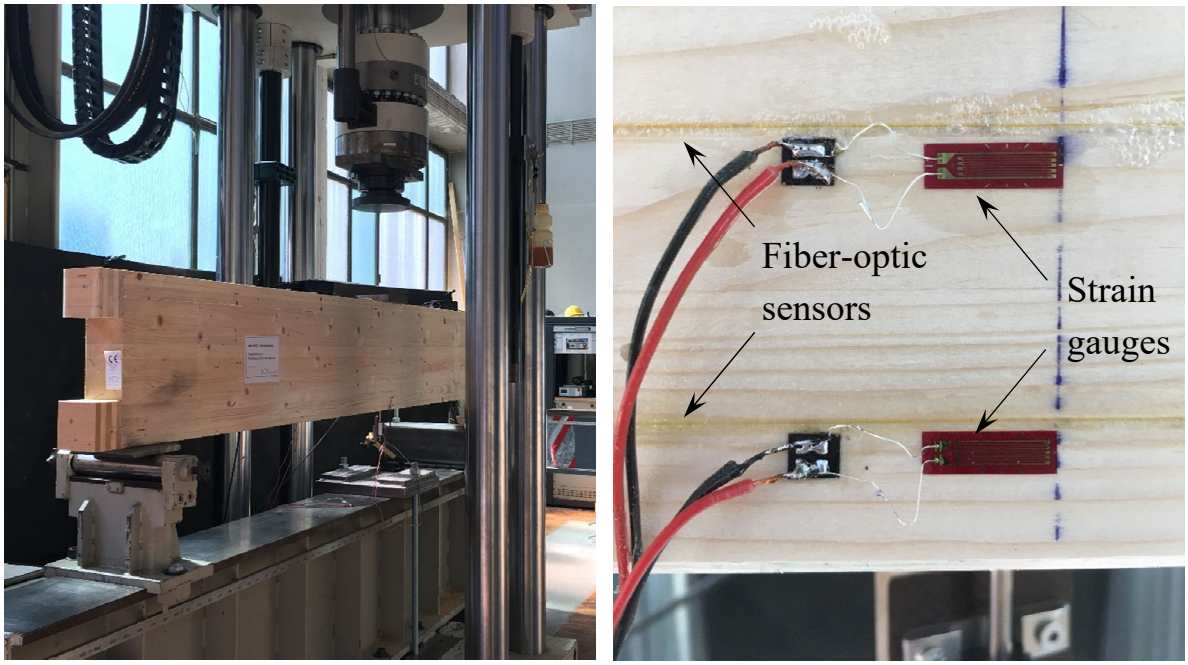

a) *b)*

Fig. 3: Fotos of the test set-up: (a) Specimen in the testing machine, (b) Detail of the sensors

The loading protocols employed for the tests are depicted in Fig. 4. First stepwise ramp-loading tests with three target load levels F_i 10, 20 and 30 kN were performed, corresponding to maximum bending tension levels at mid-span of $\sigma_{m,max} \approx 2$, 4 and 6 N/mm², respectively. The load levels were chosen to represent the linear elastic range at a level of less than 20% of the nominal characteristic GLT strength. The test was conducted in a servo-hydraulic testing machine in displacement control with a speed of 3 mm/min. At each load level F_i, the compression cylinder was stopped for t = 30 s before unloading was performed with the same speed.

Finally a short-term creep test was performed with one ramp-loading step in displacement control to F = 30 kN (with a speed of v = 3 mm/min), corresponding to a maximum bending stress of $\sigma_{m,max} \approx 6$ N/mm² at mid-span. After reaching the target load, the machine was switched to load control and the load was maintained for t = 1800 s (30 min).

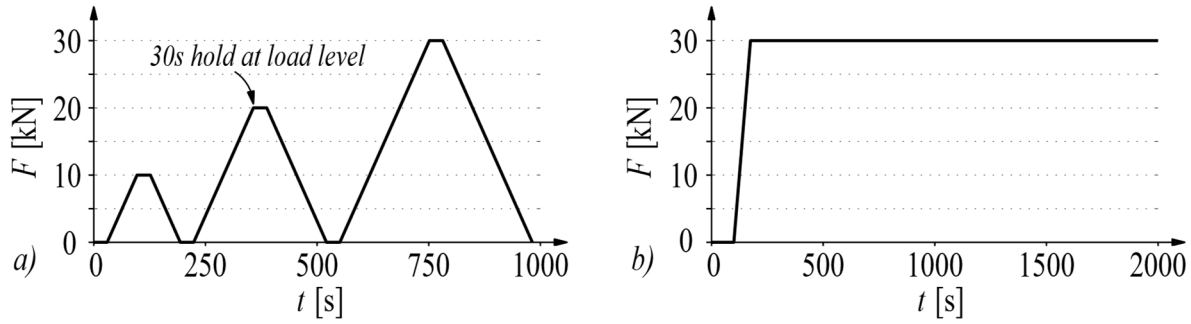

Fig. 4: Loading protocols for the ramp load tests (a) and the short-term creep test (b)

3. PRELIMINARY RESULTS

3.1 Strain distributions

From the huge amount of data stored for each load step a variety of evaluations could (and will) be performed. In this paper, only very few first evaluations are presented.

As an example for the high spatial resolution and the hereof resulting correlations between strain distribution and local wood or timber structure the strain distributions, i.e. the strains ε_x as a function of the length dimension x, are plotted in Fig. 5 for the load level F = 30 kN. The results are given for the two outer laminations in the tensile zone (i.e. laminations 3 and 4) at both side faces of the GLT beam (in black: face A and in grey: face B). In order to compare the measured strain values with the wood structure in the respective lamination, the location and the size of visible knots at the side face and the location of visible fibre deviations (i.e. wood fibre direction deviating from the beam axis due to local growth disturbances) are given in Fig. 5 as symbols at the respective locations for the respective faces A and B and the laminations 3 and 4.

The shape of the strain profile is very roughly characterised as the expected triangle shape due to the 3-point bending configuration. However, the strain distribution is to a great extent influenced by the knots and fiber deviations at the respective side faces. Some knots are only visible on one side face (see e.g. the 3rd and the 4th knot from the left side of B3) and not on the opposite side face (e.g. the respective positions for A3): The corresponding strain profiles show pronounced peaks at the knot locations of B3 and smooth behaviour without any peaks at the respective positions of the opposite face A3. Moreover, all four profiles show irregularities in the support areas of the beam, as clearly visible peaks occur next to the edges of the supporting steel plates at x = 0,2 m and 3,3 m. The presented strain profiles prove the capability of the fiber-optic measuring technology to capture the strain state of large-scale elements along multiple segments and deliver data on the *global* deformation behaviour that is easy to interpret.

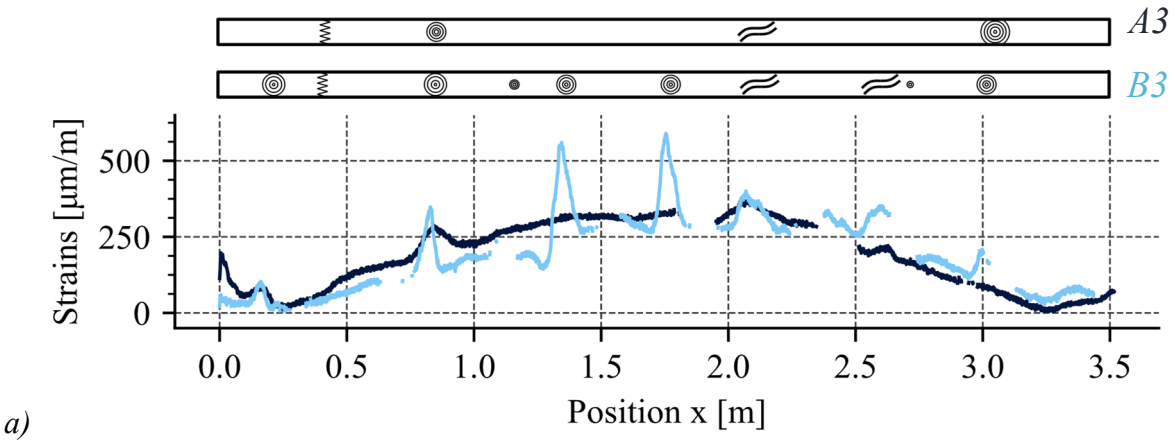

a)

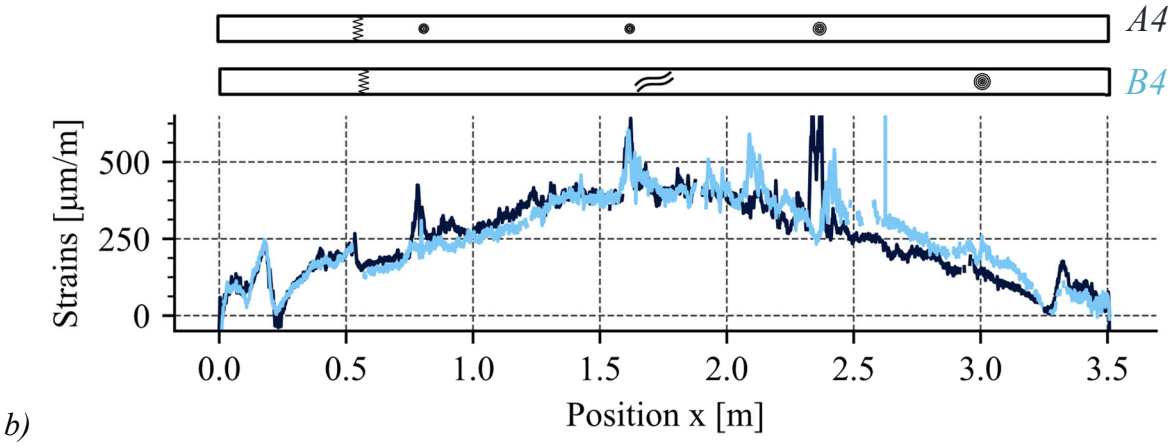

b)

Fig. 5: Strain distributions for the second-outermost lamination (a) and the outermost lamination (b) in the tensile bending zone compared to position of growth defects (knots and inclined wood fibers at load level F = 30 kN

Complementary, the detail shown in Fig. 6 demonstrates the at the same time very high spatial resolution of the employed fiber-optic sensor enabling millimeter-precise detection of *local* strain events. It is depicted the sensor situation at the third knot of lamination A4 and the spatially matched strain profile of the exact segment. As can be seen, the fiber-optic sensor passes just next to the knot. However, a clearly visible deviation in wood fiber direction of about 30 ° is apparent at about 25 mm before the centre of the knot, which is exactly where the measured strain starts to increase. Then, along the side of the knot, strain stays at roughly 500 µm/m. Just after the knot, the sensor passes through another sudden change in fiber direction even more pronounced than the first with well over 45 °, which is directly reflected in the strain profile with a strain peak of nearly 1000 µm/m. Subsequently, wood fiber direction runs nearly parallel to the fiber-optic sensor again and thus, strain levels drop to pre-knot levels again. The presented detail demonstrates in very practical manner the dependency of the elastic modulus of wood on the fiber angle and the immediate effect on the local deformation behaviour in the form of varying strain rates.

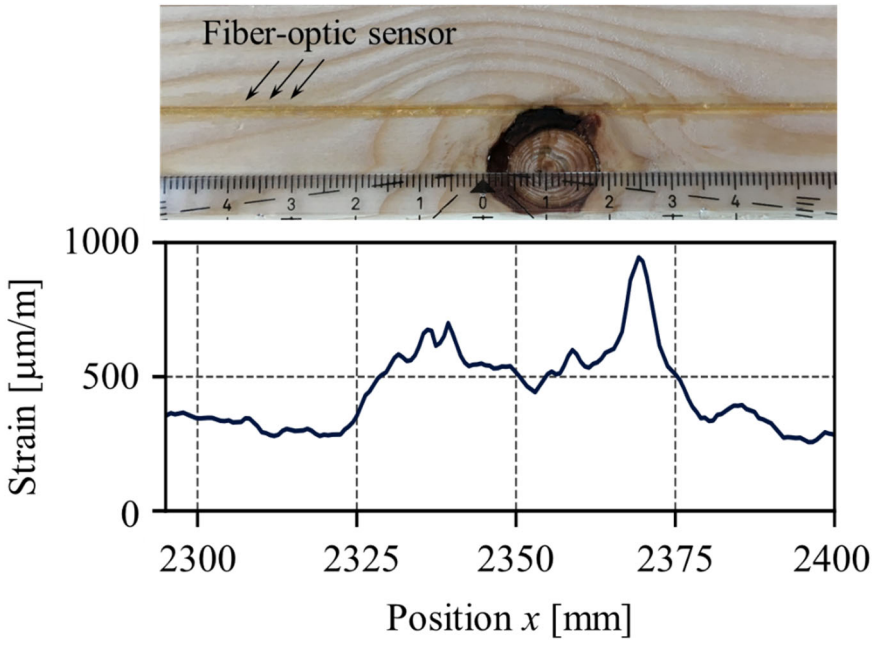

Fig. 6: Detail: Strain distribution around the third knot of lamination A4

3.2 Results of optical fiber sensors and electronic strain gauges

In order to verify the optical strain measurements in a quantitative manner a direct comparison between the strain data extracted from the optical fibre data with data from usual electronic strain gauges has been performed. As described in section

2 the optical fibre sensor and the strain gauges were located directly side by side at the same length position $x_{FOS} = x_{strain\ gage}$. For the comparison the FOS strain data were integrated over the length of the measuring grid of the strain gauges. Table 1 contains the strain results of both measuring methods and the percentage of deviation between the two methods, whereby the long-proven measuring principle of electronic strain gauges has been considered as the reference method. The percentage deviations were not more than about 5%, which verifies the validity of the FOS strain data not only in a qualitative manner, but also with respect to absolute numbers.

Table 1: Strain results at F = 30 kN: comparison of optical and electronic measurements

Location	*Position x [mm]*	*Strain FOS (opt. fiber) [µm/m]*	*Strain ESG (electr. gauge) [µm/m]*	*Deviation /(FOS – ESG)/ESG [%]*
A3	1750	315	331	5,1
A4	1750	396	397	0,3
B3	1145	185	193	4,3
B4	1145	277	288	4,0

3.3 Time-dependent behaviour

In order to illustrate the first results of the short-term creep test (constant load of 30 kN for 1800 sec) three different positions on one lamination (B3) have been chosen, which are representative for the different time-dependent behaviour of different structures: Fig. 7a gives the three selected positions, where the time dependent strain evolutions have been evaluated.

Fig. 7b gives the strain results, which have been evaluated from the recorded FOS-data at the three chosen positions:

- Position I: Directly next to the knot the strain is clearly decreasing with time, i.e. relaxation is observed.
- Position II: At this position at virtually “defect free” wood the strain is increasing with time, i.e. the expected creep behaviour of the viscoelastic material is observed.
- Position III: At this position with visible inclined wood fibres the strain is approximately constant, i.e. no clear tendency of creep or relaxation is observed.

The chosen three positions are representative for all laminations: For all knots clear relaxation is observed, whereas the adjacent defect free show creep behaviour. When evaluating the whole lamination length in a sum, the areas without knots dominate the overall behaviour: Thus, the resulting global behaviour is creep, observed as increasing deflection with time.

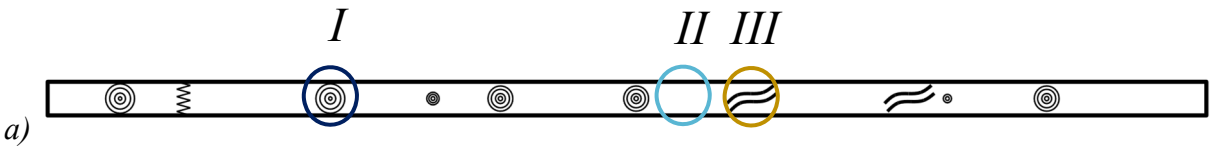

a)

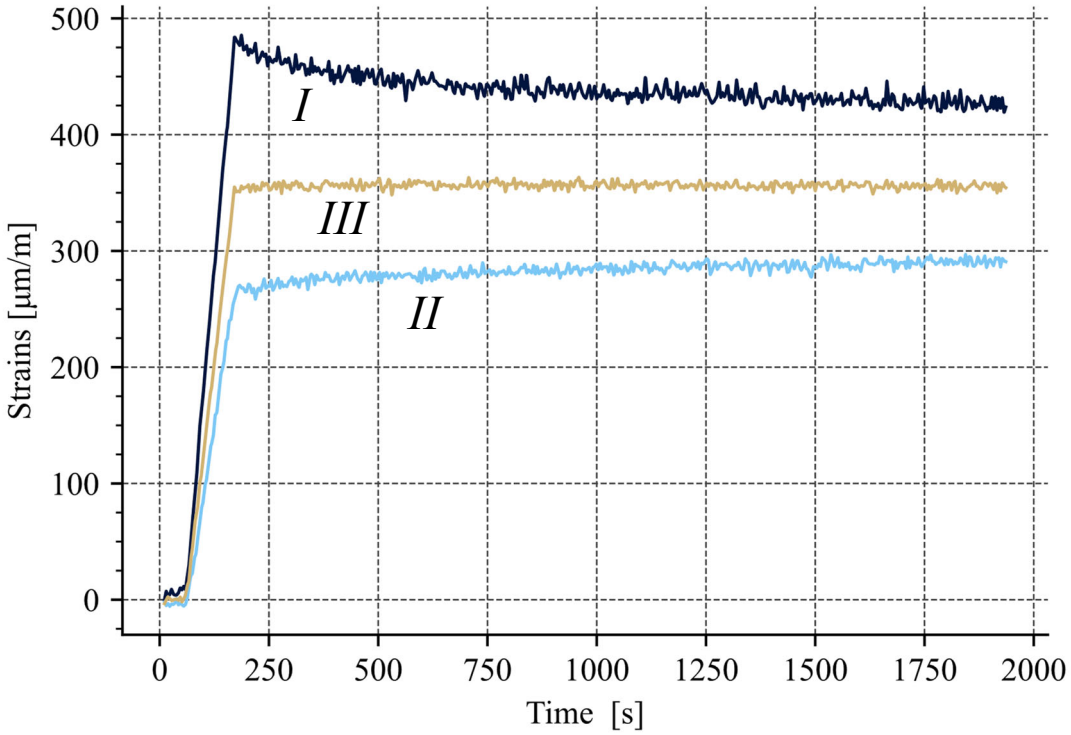

b)

Fig. 7: Time dependent evolution of localized strain (b) at 3 different positions I, II and III (a)

The somewhat surprising result of relaxation in the vicinity of knots – at global creep behaviour – can preliminary be explained as follows: Although the global loading and boundary conditions represent a creep test, i.e. a constant load is applied to the specimen and the specimen (the GLT beam) deforms dependent on the loading time. However, within the GLT cross-section the boundary conditions have to be described differently: as the beam cross-sections are always plane (acc. to Bernoulli assumption), the boundary condition in the GLT cross-section can be described by an even strain distribution. In that case the stresses are transferred

from localised zones with higher creep rates – such as the knots or the area directly located to the knots – to zones with lower creep rates – such as “defect free” clear wood”. This behaviour results in an “unloading” of the knots showing up in the local FOS measurements by locally decreasing strain. The load transfer to the clear zones shows up by increasing strain values.

The first measurement data have to be evaluated in more detail and the given mechanical interpretation of the results in the short-term creep test have to be confirmed quantitatively by numerical modelling. However, it can already be stated, that the strain measurement of timber and GLT at full size level with extremely high spatial resolution and high strain exactness gives a valuable insight into the mechanics of solid timber engineered products, which has not been possible to that extent with other strain measurement techniques.

4. CONCLUSIONS AND OUTLOOK

The results of the first preliminary tests with fiber-optic strain measurements at a full size GLT beam show the feasibility of the technique and underline the advantages of the method: Wide coverage of large structural members with extremely high spatial resolution measured with sufficient high capture rate. The accuracy of the strain measurement was verified by comparison with conventional electronic strain gauges positioned directly next to the fiber-optical sensors. The strain profiles give deeper insight into the very uneven strain distributions of common quality timber with growth defects such as knots and inclined wood fibres. The short-term creep test yielded some unexpectedly pronounced relaxation behaviour in the vicinity of knots.

In the next step of the research project the non-linear behaviour at higher load levels in the tensile and the compression zone is being investigated. The method will be applied to critical sections in timber structures such as holes or joints. Furthermore, the influence of moisture and temperature changes and the interaction with loading time have to be characterised. Finally, criteria for identification of damage related strain – in contrast to elastic, moisture-, temperature- and creep-related strain components – will be developed as a foundation of a strain-based monitoring system.

ACKNOWLEDGEMENTS

It is gratefully acknowledged that the ZIM project "Dehnungsbasiertes Schadensmonitoring für hochbelastete Holzbauteile (desmo.WOOD)" with the project ID 16KN094639 is funded by the Federal Ministry for Economic Affairs and Climate Protection based on a resolution of the German Bundestag within the framework of the ZIM research network "InnoBauHolz". We also would like to thank our project partners University of Cooperative Education Sachsen, Dresden, company STRAB Ingenieurholzbau Hermsdorf GmbH, Hermsdorf, company Trans4mation IT GmbH, Dresden and the project executing agency VDI/VDE Innovation+Technik GmbH, Berlin.

REFERENCES

[1] SAKIYAMA, F.I.H., LEHMANN, F., GARRECHT, H.: *Structural health monitoring of concrete structures using fibre-optic based sensors: a review*. Magazine of Concrete Research 73 (4), 2019, pp. 174-194

[2] CLAUS, T., SEIM, W., KÜLLMER, J.: *Force distribution in self-tapping screws: experimental investigations with fibre Bragg grating measurement screws*. European Journal of Wood and Wood Products 80, 2022, pp. 183-197

[3] FRANKE, S., MAGNIÈRE, N., SCHIERE, M., FERRAZZINI, T., MEIER, C., BOSSEN, A.: *Einsatz von FBGS im Holzbau – Development and use of optimized Fibre Bragg Grating sensors for long term monitoring of timber components*. Research report, Bern University of Applied Sciences, 2016

[4] MARSILI, R., ROSSI, G., SPERANZINI, E.: *Fibre Bragg Gratings for the Monitoring of Wooden Structures*. Materials 11 (7), 2018, https://doi.org/10.3390/ma11010007

[5] SAMIEC, D.: *Verteilte faseroptische Temperatur- und Dehnungsmessung mit sehr hoher Ortsauflösung*. Photonik 6, 2011, pp. 34-37

[6] SCHMIDT-THRÖ, G., SCHEUFLER, W., FISCHER, O.: *Kontinuierliche faseroptische Dehnungsmessung im Stahlbetonbau*. Beton- und Stahlbetonbau 111 (8), 2016, https://doi.org/10.1002/best.201600026

[7] HENAULT, J.M., SALIN, J., MOREAU, G., DELEPINE-LESOILLE, S., BERTAND, J., TAILLADE, F., QUIERTANT, M., BENZARTI, K.: *Qualification of a truly distributed fiber optic technique for strain and temperature measurements in concrete structures*. EPJ Web of conferences 12, 2011, https://doi.org/10.1051/epjconf/20111203004

[8] TEGUEDY, M.C., JOLY-LAPALICE, C., SORELLI, L., CONCIATORI, D.: *Optical fiber sensors implementation for monitoring the early-age behavior of full-scale Timber-Concrete Composite slabs*. Construction and Building Materials 226, 2019, pp 563-578

[9] FROHNMÜLLER, J., SEIM, W., SPANGENBERG, A.: *Fibre-optic measurements for monitoring adhesively bonded timber-concrete composite beams*. Conference Paper, World Conference on Timber Engineering, Oslo, Norway, 2023, pp. 750-758

[10] JOCKWER, R., GRÖNQUIST, P., FRANGI, A.: *Long-term deformation behavior of timber columns: Monitoring of a tall timber building in Switzerland*. Engineering Structures 234, 2021, https://doi.org/10.1016/j.engstruct.2021.111855

[11] EN 14080, *Timber structures – Glued laminated timber and glued solid timber – Requirements; German version EN 14080:2013*. European Committee for Standardization, Brussels, Belgium, 2013